

Instability of a coastal jet in a two-layer model ; application to the Ushant front

Marc Pavéc (1,2), Xavier Carton (1), Steven Herbette (1), Guillaume Roulet (1), Vincent Mariette (2)

(1) UBO/LPO, 6 av. Le Gorgeu, 29200 Brest, France ; (2) Actimar, 24 quai de la Douane, 29200 Brest, France ;
xcarton@univ-brest.fr

Abstract :

The instability of a shelf front, with the characteristics of the Ushant front (steep density gradient and narrow jet), is investigated on the f -plane within the framework of a two-layer shallow-water model. Linear stability analysis and nonlinear numerical simulations show that baroclinic waves, with 20 and 40 km wavelengths, are the most unstable ones, with growth rates on the order of $(1\text{day})^{-1}$, which is comparable to what is observed on SST images. The analysis of growing perturbations in a two-layer primitive equation model (MICOM) shows that the latter are vertically shifted, which corroborates that the governing mechanism for the generation asymmetric meanders and eddies in our simulations, is baroclinic instability. Then, in order to take into account tidal effects, we add a time-periodic barotropic mean flow. Although we succeed observing some characteristics of parametric resonance (frequency selection, stepwise growth), baroclinic instability remains the main mechanism to explain the growth of meanders.

Key-words :

Frontal jet, baroclinic and parametric instability

1 Introduction

The baroclinic instability of coastal jets, and in particular of frontal currents (defined here as currents associated with density fronts), has been the subject of recent studies (e.g. Boss *et al.* (1996)). This instability leads to the growth of waves with length comparable to 2π times the internal radius of deformation. If the lower layer outcrops at the front, instability also occurs on a separate band of shorter waves ; this mechanism was related to the interaction of Rossby and Kelvin modes (Sakai (1989)). If the mean velocity of the jet varies periodically with time (due to a variation of transport, for instance), parametric instability can also occur ; several studies in a idealized framework evidenced its predominance near the curve of marginal baroclinic instability (Pavéc and Carton (2004), Pavéc *et al.* (2005), Pavéc *et al.* (2006)).

An interesting example of coastal jet which can a priori develop both baroclinic and parametric instability is the Ushant front. This density front separates thermally stratified water masses west of $5^{\circ}20'W$ from tidally-mixed, homogeneous water masses east of this longitude. Observations, both from satellite and in-situ, provide information on this flow : the temperature difference at the surface is $2 - 3^{\circ}C$ over 5km distance (the frontal jet width), the associated currents are on average 0.2-0.3m/s, the internal deformation radius near in the stratified zone is close to 6km, and this front undergoes a semi-diurnal tidal forcing with velocities that can reach 2m/s. Meanders with about 40km wavelength and filaments with about 20km cross-section are observed on this front (see figure 1 (left)).

The objective of the present work is to determine if a simple two-layer shallow-water model, initialized with a slightly perturbed narrow jet, can reproduce the observed characteristics of the instability and if the interaction of the perturbation with a periodic barotropic mean flow (mimicking the tidal forcing) can lead to parametric resonance.

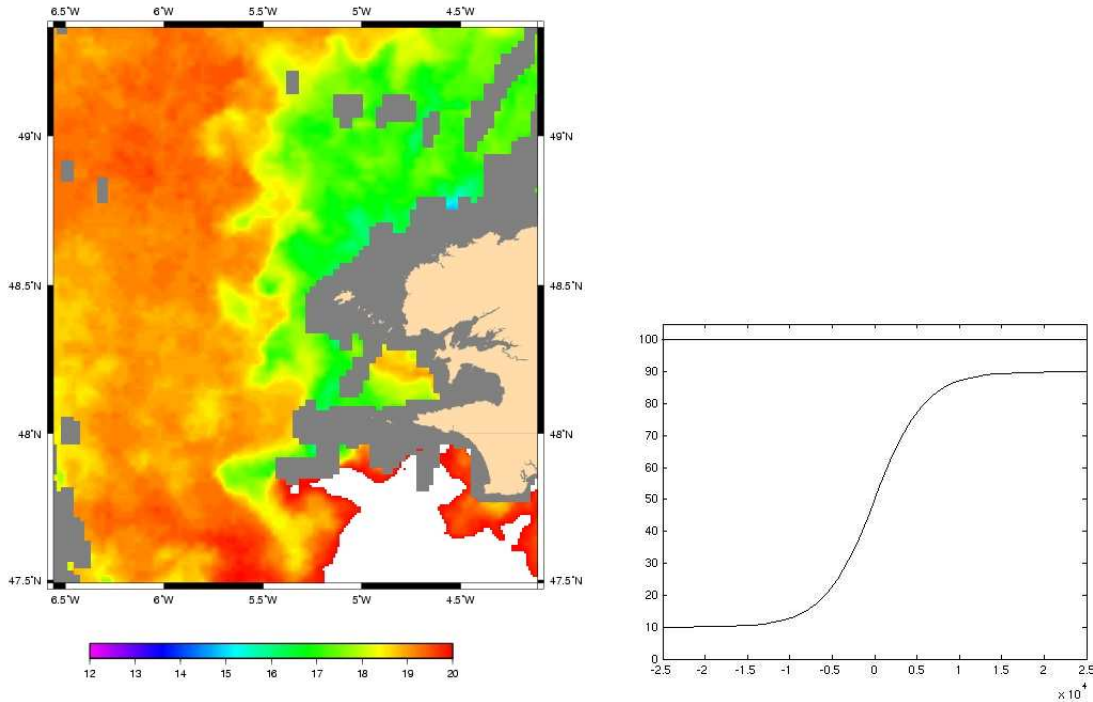


Figure 1: (left) SST in the Irish Sea on July 24, 2006 ; (right) average density structure of the front

2 Baroclinic instability of the frontal flow

A two-layer shallow-water model is chosen to allow strong isopycnal deviations (see figure 1 (right)). For this preliminary study, a f-plane hypothesis is chosen in reason of the small latitudinal extent of the flow. The dynamical equations are

$$\partial_t u_j + (\vec{u}_j \cdot \vec{\nabla}) u_j - f_0 v_j = -\partial_x P_j \quad (1)$$

$$\partial_t v_j + (\vec{u}_j \cdot \vec{\nabla}) v_j + f_0 u_j = -\partial_y P_j \quad (2)$$

$$\partial_t h_j + \vec{u}_j \cdot \vec{\nabla} h_j + h_j \vec{\nabla} \cdot \vec{u}_j = 0 \quad (3)$$

with $j = 1, 2$ the upper, lower layer index. A consequence of these equations is the conservation of potential vorticity $q_j = (\partial_x v_j - \partial_y u_j + f_0)/h_j$. The mean flow is purely baroclinic $U_1(y) = -U_2(y)$, zonal (rotated by 90 degrees with respect to the ocean) and in geostrophic balance.

$$U_1 = -\frac{1}{f} \frac{dP_1}{dy} = -\frac{g}{f} \frac{d}{dy} (h_1 + h_2) \quad (4)$$

$$U_2 = -\frac{1}{f} \frac{dP_2}{dy} = -\frac{g}{f} \frac{d}{dy} \left(h_1 + h_2 + \frac{\Delta\rho}{\rho} h_2 \right) \quad (5)$$

leading to upper and lower layer thicknesses h_1 and h_2 , in the steady state, defined by

$$h_1 = H_1 - \frac{1}{1 - \Delta\rho/2\rho} \frac{\Delta h}{2} \tanh\left(\frac{y}{\sigma}\right) \quad (6)$$

$$h_2 = H_2 + \frac{1}{2} \Delta h \tanh\left(\frac{y}{\sigma}\right) \quad (7)$$

To be consistent with the characteristics of the Ushant front, we choose $H_1 = 50m, H_2 = 50m, \Delta h = 80m$. Furthermore, $\Delta\rho = \alpha\rho\Delta T$, with $\alpha = 1.79 \cdot 10^{-4} K^{-1}$. In the reference case, $\Delta\rho/\rho = 7 \cdot 10^{-4}$ and $\sigma = 5km$. The domain is a zonally periodic square basin

of $100\text{km} \times 100\text{km}$.

In the linear analysis, equations (1-2-3) are linearized around the mean flow (4-5) with a normal mode perturbation of the form $(u'_j, v'_j, p'_j, h'_j) = (u'_{j0}, v'_{j0}, p'_{j0}, h'_{j0})(y)e^{ik(x-ct)}$ and boundary conditions for the perturbation are no normal flow at the northern and southern boundaries. The resulting matrix problem is solved with a generalized eigenvalue-eigenvector method.

The nonlinear equations are solved numerically with the MICOM model (Bleck and Boudra (1981), Bleck and Boudra (1986), Herbette et al. (2004)); the horizontal grid size is 1km and we set the Smagorinski coefficient of the biharmonic horizontal dissipation operator to 0.1.

2.1 Reference case

The values of the parameters given here-above lead to a baroclinic velocity on the order of 0.275m/s, quite compatible with measurements performed across the Ushant front (Mariette (1983)), and fall in the range of baroclinic instability as suggested by linear stability analysis. Numerical simulations, in which we initially add a small amplitude white-noise disturbance to the mean flow, show growing meanders and formation of eddies (See lower layer potential vorticity maps from day 11 to day 14 in figure 2). The growth of meanders and the wrapping

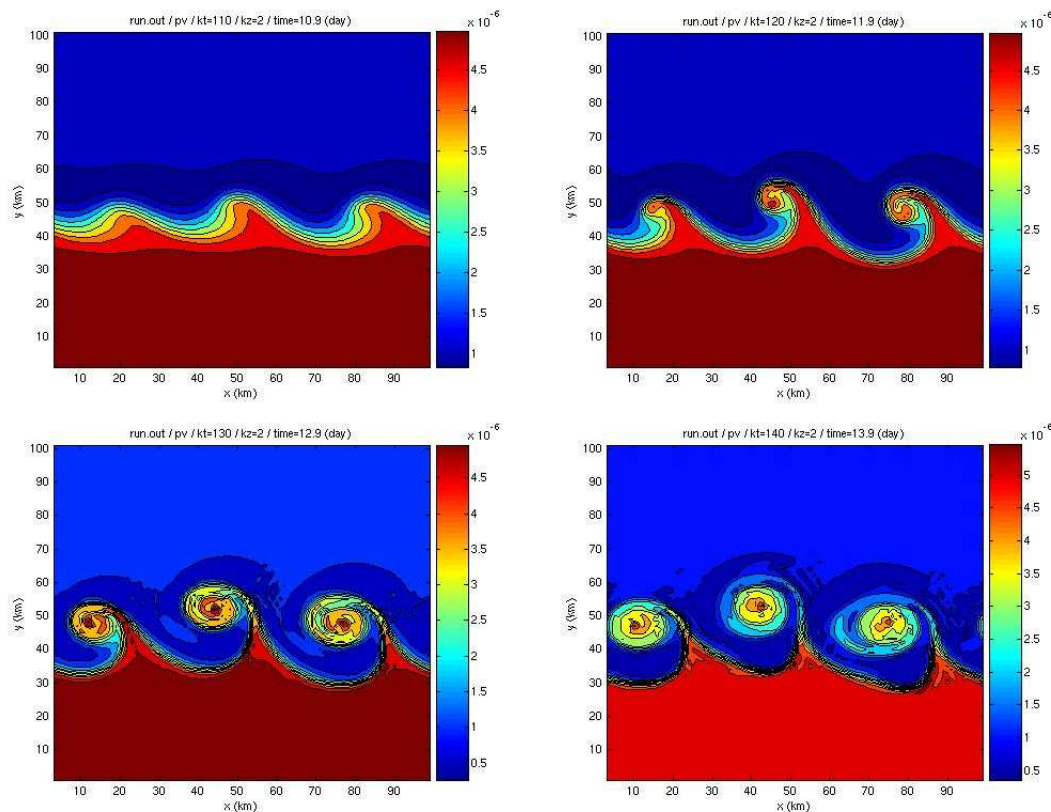


Figure 2: Potential vorticity maps in the lower layer from day 11 to day 14

up of their tip leads to eddy formation. Though initially, a wavelength close to 30km seems to dominate, the front becomes irregular after a few days, indicating the presence of other wavelengths. Indeed, a spectral analysis of the perturbation in zonal modes indicates that mode 2 grows nearly as fast as mode 3, but to a smaller amplitude, and that mode 1 becomes large once the vortices have formed (see figure 3). The baroclinic nature of the instability is confirmed

by the vertical phase shift between the layer perturbations of potential vorticity (shown in Pavéc (2007)).

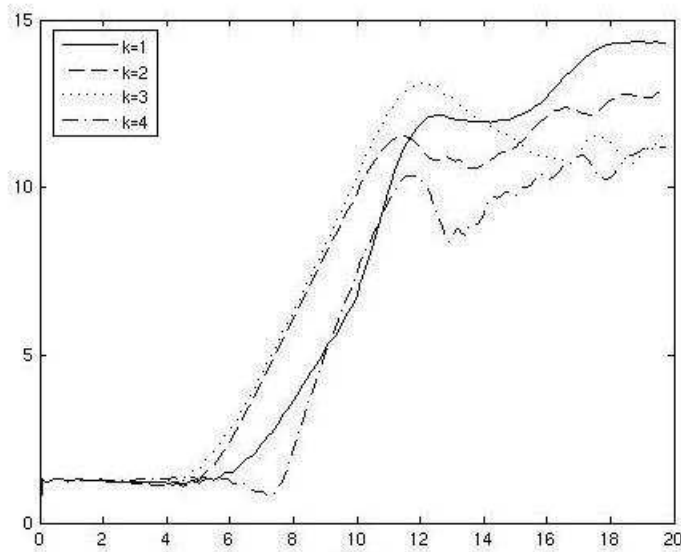


Figure 3: Spectral analysis of potential vorticity (PV) in the reference case : the log of the meridionally averaged PV of each mode is plotted with respect to time (in days)

2.2 Sensitivity study

This part shows how sensitive are the growth rates of modes 1-2-3 to both the width of the front σ and the density jump $\Delta\rho$. If $\Delta\rho$ is kept constant and σ increases, growth rates decrease (figures shown in Pavéc (2007)). Conversely, growth rates increase; in both cases, the baroclinic velocity varies. Now if the baroclinic velocity is kept constant and equal to about 0.275 m/s, σ is proportional to $\Delta\rho$ in a good approximation. Figure 4 shows that the growth rates decrease with increasing σ in this case, and thus the width of the front is the dominant parameter in this evolution.

A series of nonlinear simulations (for a front width varying between 2 and 20km) shows that too narrow a front leads to a very regular spacing of meanders (with a dominant mode 3 of perturbation) while too wide a front leads to too slow a growth of these meanders. A front width of 5km leads to results closer to observations, in particular two dominant modes with 30 and 50km wavelengths, comparable to the observed 20 and 40km spacing of meanders and filaments. Our simulations also indicate that, as the front is less marked, the wavelength increases, a feature indeed observed on the Ushant front in spring.

3 Parametric resonance

Since tidal flow influences the Ushant front, we study here the influence of an oscillatory, barotropic mean flow on the stability of our idealized baroclinic current. Three different amplitudes, 0.02, 0.2 and 2m/s, and seven periods, ranging from 6 to 12 hours, are tested for this oscillating barotropic mean flow. Theory (e.g. Pavéc *et al.* (2005), Pavéc *et al.* (2006)) indicates that parametric instability of coastal currents is most effective near the curve of marginal baroclinic instability. The resonant period is then given by the pulsation of the marginal baroclinic wave.

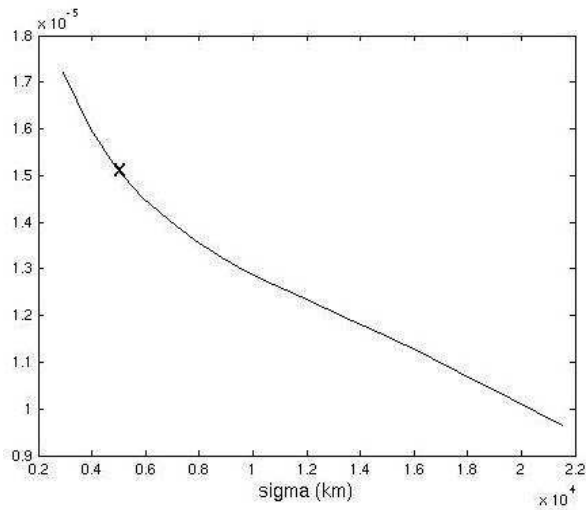


Figure 4: Growth rates (in seconds⁻¹) with respect to the width of the front for a baroclinic mean velocity set equal to 0.275 m/s

Here, for a realistic choice of flow parameters, nonlinear simulations lead to the following results : whatever the choice of oscillatory flow amplitude, the growth rates previously obtained for baroclinic instability are not considerably altered. Nevertheless, for a finite range of periods of oscillatory flow, the growth of the perturbation has a steplike evolution with time (see modes $k = 1, 3, 4$ on figure 5) ; this effect is most marked for the 9h period whereas linear calculations suggest a peak of resonance at the 7h period. Frequency selection and steplike growth are characteristic of parametric resonance. But the influence of parametric resonance remains moderate here because for realistic flow conditions, baroclinic instability is dominant.

4 Conclusions

The objective of this study was to analyze possible mechanisms leading to the growth of short waves on a shelf front in an idealized model, with application to the Ushant front. In fact, for the latter, satellite observations of SST, show meanders and filaments at 20 to 40 km spacing. Numerical simulations, with a two-layer shallow-water model, of the evolution of a narrow shelf jet in geostrophic balance, was able to reproduce the growth of meanders and eddies with similar sizes as those that are observed for the Ushant front. The width of the front appears to be the key parameter that governs its evolution. The analysis of the vertical phase shift of the growing perturbations confirmed that the governing mechanism was baroclinic and frontal instability. Within the range of realistic parameters values, the presence of an oscillatory barotropic mean flow was not able to trigger another type of instability, and baroclinic instability always remained the dominant process. Nevertheless, we could observe some signs of parametric resonance: frequency selection and step like growth.

A first step towards more realism after this study should consider a meridional mean flow on the beta-plane; indeed, the beta-effect would then favor the zonal growth of perturbations. In a second step, realistic stratification, bathymetry and forcing should also be included.

References

Bleck, R., Boudra, B. 1981 Initial testing of a numerical ocean circulation model using a hybrid

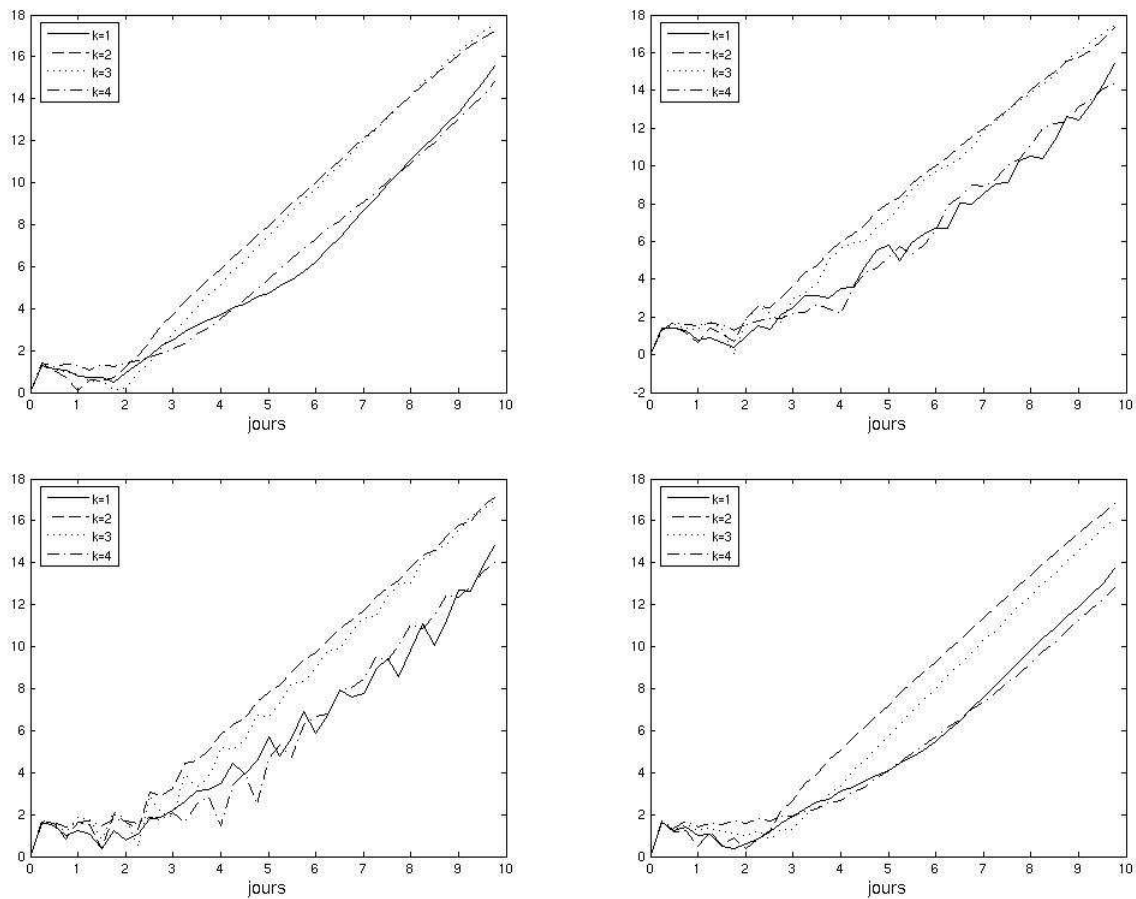


Figure 5: Growth of the first four modes ($k=1,2,3,4$) with respect to time (in days) for a barotropic oscillatory flow of 2m/s with periods of 6, 7, 9 and 12 hours ; as in figure 3, the modal amplitude is the logarithm of meridionally averaged PV.

- (quasi-isopycnic) vertical coordinate *J. Phys. Oceanogr.* **11** 755-770.
- Bleck, R., Boudra, B. 1986 Wind-driven spin-up eddy resolving ocean models formulated in isopycnic and isobaric coordinates. *J. Geophys. Res.* **91** (C6), 7611-7621.
- Boss, E., Paldor, N., Thompson L. 1996 Stability of a potential geostrophic front: from quasi-geostrophy to shallow-water, *J. Fluid Mech.* **315** 65-84
- Herbette, S., Morel, Y., Arhan, M. 2004 Subduction of a surface vortex under an outcropping front *J. Phys. Oceanogr.* **34** 1610-1627.
- Mariette, V. 1983 Effets des échanges atmosphériques sur la structure thermique marine; application à des zones du large et à une zone côtière *Thèse de Doctorat, Université de Bretagne Occidentale*
- Pavec, M., Carton, X. 2004 Parametric instability of a two-layer wall jet *Reg. Chaot. Dyn.* **9** 499-508
- Pavec, M., Carton, X., Swaters, G. 2005 Baroclinic instability of frontal geostrophic currents over a slope *J. Phys. Oceanogr.* **35** 911-918
- Pavec, M., Carton, X., Poulin, F. 2006 Parametric instability of boundary currents in a two-layer QG model *Dyn. Atmos. Ocean* **submitted**
- Pavec, M. 2007 Instabilités barocline et paramétrique des courants de bord ; application au front d'Ouessant *Manuscrit soumis à thèse de Doctorat, Université de Bretagne Occidentale*
- Sakai, S. 1989 Rossby-Kelvin instability : a new type of ageostrophic instability *J. Fluid Mech.* **202** 149-176